Two-Phase Flow Performance for Electrical Submersible Pump Stages

Rui Pessoa, SPE, PDVSA-Intevep, and **Mauricio Prado,** SPE, U. of Tulsa

Summary

Two-phase flow behavior prediction for centrifugal pumps is a difficult task because of the complexity involved in modeling multiphase flow inside turbo machines. An experimental study has been conducted at the U. of Tulsa Artificial Lift Projects (TUALP) with a 513-series, 22-stage, mixed-flow-type pump to gather data for pump performance under two-phase flow conditions. Air and water were used as the working fluids. This study differs from other experimental works because the pressure changes were recorded stage by stage. The results of previous works have been reported as an average of the intake and discharge conditions and depend on the number of stages used.

Phenomena such as surging and gas locking were observed during these tests, and their boundaries have been mapped.

The pressure increment and total hydraulic horsepower for the average pump, those per stage as a function of the liquid flow rate, and each gas flow rate considered are presented. The pump's average brake horsepower and efficiency also are plotted for the variables mentioned.

The results indicate that average pump behavior is significantly different from that observed per stage.

Introduction

Centrifugal pumps are dynamic devices that use kinetic energy to increase liquid pressure. They are successful when handling water and other incompressible fluids, ranging from low to medium viscosities, but are severely impacted by free gas or highly compressible fluids.

Significant amounts of free gas may be found during hydrocarbon production. This motivated important research from the petroleum industry that focused on improving the successful application of electric submersible pumps (ESPs) as an artificial lift method.

The consequences of entrained gas on centrifugal pumps depend on the relative amount of gas and liquid present and vary from a slight performance deterioration to a complete blockage, known as "gas locking." Before gas locking occurs, another phenomenon, known as surging, takes place.

Each pump is characterized by performance curves that include the head developed, the brake horsepower consumed, and the efficiency as a function of the flow rate through the pump for a certain rotational speed (see **Fig. 1**). Traditionally, these curves are determined experimentally with water.

The head's characteristic curve is used to size the pump, while the brake horsepower information assists in sizing the motor required to drive the pump. The sizing of a multistage ESP for water wells is fairly simple, and good accuracy of the predicted performance is achieved with the water performance information supplied by the manufacturer.

ESP system design with the water information for oil wells with a high free-gas fraction at pump intake conditions is a harder task, based on predicting performance curves by modifying the water curves. The leading parameter is the mixture density at the flow conditions of each stage. By applying this procedure, the ESP system often shows some degree of under- or oversizing when operating.

This paper (SPE 81910) was revised for publication from paper SPE 71552, first presented at the 2001 SPE Annual Technical Conference and Exhibition, New Orleans, 30 September–3 October. Original manuscript received for review 27 November 2001. Revised manuscript received 23 September 2002. Paper peer approved 5 November 2002.

Accurately predicting the performance of any pump that handles free gas is challenging, and some empirical and mechanistic approaches have been attempted in the past. The main problem with the experimental approach is that the correlations developed are based on average pump performance and become specific for the type and number of stages tested. On the other hand, theoretical models are difficult to develop because the geometry of the channels inside the pump is complex. The phenomena that take place in such channels are not well understood, and, thus, using empirical parameters is required to close the model.

Additionally, ESPs also need prediction for surging and gas-lock conditions to head degradation when handling free gas.

One major contribution of experimental studies is identifying the main parameters that rule centrifugal pump behavior when handling gas. These parameters seem to be the pump intake pressure, the volumetric fractions of free gas and liquid phases, the liquid flow rate, and the angular speed.

In this work, an experimental study was conducted that focused on these same parameters while measuring the pump performance per stage. With respect to earlier experimental works, the main contribution of the present study is elimination of the specific limitation of correlations based on averaged data.

Literature Review

This section focuses mainly on works published by the petroleum industry with some references from the nuclear industry.

The first part is devoted to discussing and analyzing each work as well as the traditional method employed to predict pump performance under two-phase flow. Fundamental concepts are introduced afterward, because they are required to better understand two-phase flow behavior in centrifugal pumps. A standardization of the Nomenclature and definitions must be conducted in future works to establish a common base for comparing these methods. For this reason, a comparative analysis of previously discussed studies is presented.

Traditional Method of Head Performance—Homogeneous Model. For incompressible single-phase fluids at a known intake pressure and temperature, the pressure increment developed by a specific ESP stage is a function of the flow rate and the density.

$$\Delta p = \Delta p(q_l, \rho_l). \quad (1)$$

For low-viscosity liquids, the pressure increment of the ESP stage is directly proportional to the fluid density. In this way, we can define an indirect measurement of the pressure increment in terms of the head, defined as

$$H = \Delta p / g\rho_l. \quad (2)$$

This concept is very important for practical applications. For low-viscosity and incompressible fluids, the ESP-stage pressure increment can be expressed by a unique relationship of the head as a function of the flow rate but independent of the fluid density.

Because of this, ESP performance curves can be determined with any liquid that meets the specified requirements (usually water), which can be used to predict the ESP behavior with other single-phase fluids.

ESP application in oil wells is a different topic because of the multiphase conditions usually present.

The homogeneous model assumes that ESP single-phase performance curves can be used to represent two-phase behavior. In this method, the two-phase flow head delivered by the pump is equal to the single-phase liquid head at the mixture's total in-situ flow rate.

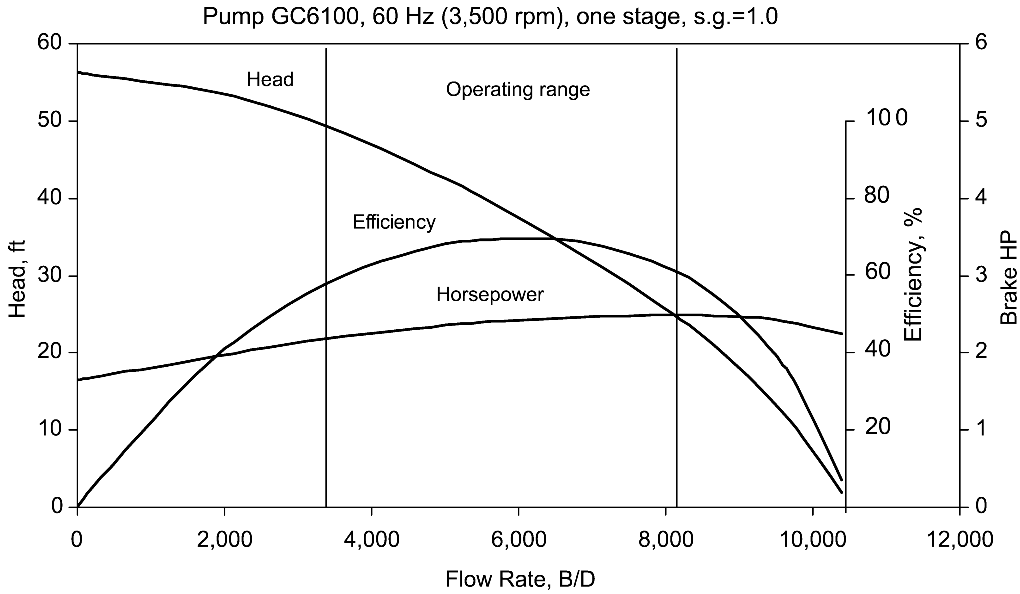

Fig. 1—Manufacturer's catalog curves.

When this procedure is applied to the whole catalog curve for different free gas percentages at the pump intake, head curves can be obtained as shown in **Fig. 2.**

Once the head developed by the first stage is determined, the discharge pressure can be computed and becomes the intake pressure for the next stage. The free-gas fraction and the total volumetric flow rate are adjusted according to the new conditions. The procedure is applied again for the next stage. The pressure increment of each individual stage is calculated with the mixture density.

$$\Delta p_{TP} = gH\rho_m. \qquad (3)$$

It can be noticed that the procedure, once carefully analyzed, does not implement any head degradation. It shifts the head points from the water curve according to the total volumetric flow rate.

In this procedure, the pump's multiphase pressure increment is expressed in terms of a mixture head that is based on the mixture density. Alternatively, this head prediction can also be expressed in terms of a single-phase water density by multiplying two-phase mixture head by the mixture's specific gravity. Doing so causes Eq. 2 to become

$$H_{TP} = \frac{gH\,\rho_m}{g\rho_w} = H\gamma_{g,m}. \qquad (4)$$

Here, the head in height of water is calculated by multiplying the original head by the mixture's specific gravity.

Applying the procedure for different free-gas percentages at the pump intake allows the head performance curves shown in **Fig. 3** to be generated.

At a simple glance, it seems that head degradation has been introduced, but from a mathematical point of view, the curves shown in Figs. 2 and 3 represent the same-stage pressure increment. The apparent difference is caused by how pressure-increment results are presented by considering either the mixture density or the single-phase water density.

The homogeneous method enabled predicting head performance when the flow can be treated as a homogeneous mixture, but no correlation was available to estimate surging and/or gas-locking limits until experimental studies were carried out. For that purpose, field experience was crucial in generating some rules of thumb. Limits of 10 and 25% free gas at the suction were established for hydraulic-radial- and mixed-flow-type pumps, respectively. These values were wrongly accepted, regardless of the pump intake pressure, until the importance of this parameter was demonstrated experimentally.

Previous Studies. Few studies are available regarding the behavior of centrifugal pumps handling two-phase mixtures. Two major industries seem to be interested in the topic, but different pump types are used. The petroleum industry is mainly concerned with multistage, small-diameter pumps (ESPs), while the nuclear industry focuses on single-stage, higher-diameter pumps.

Most of the petroleum industry's research has been of an empirical nature because of the complexity of the phenomena that

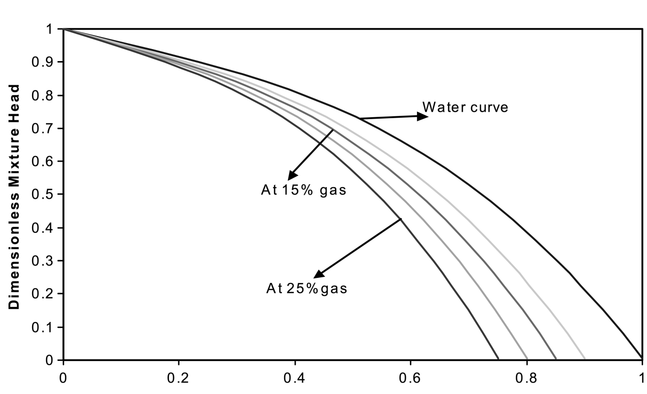

Fig. 2—Performance curves for the pump with the traditional method for the mixture density.

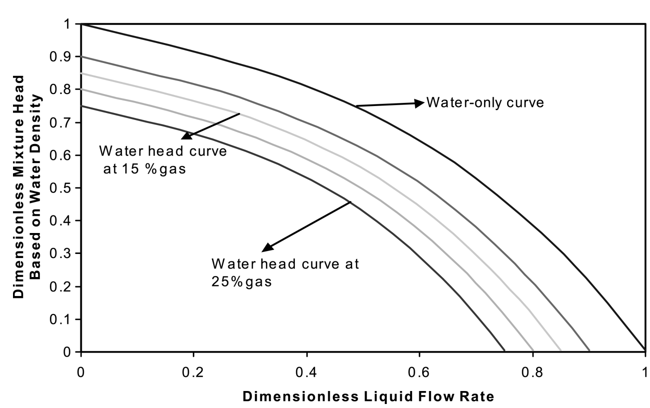

Fig. 3—Performance curves for pump with the traditional method for water density.

rule centrifugal pump behavior. The isolated experiments conducted so far have been fundamental to understanding the tendencies of and providing insight to the real behavior of ESPs when handling gassy fluids.

Lea and Bearden (1982).[1] The authors tested three different pumps—the I-42B and C-72 with radial stages and the K-70, a mixed-flow type that uses diesel-CO_2 as the two-phase mixture. The first pump was also tested with water-air. No more than eight stages were used in each case. Tests consisted of increasing the percentages of gas by volume at the pump inlet in steps until the pump failed to deliver any head (gas locking). For diesel-CO_2, the experiments were performed by varying the intake pressure between 50 and 400 psig and the intake gas percentage by up to 50%. In the case of water-air, the intake pressure ranged from 25 to 30 psig, and the intake gas percentage varied by up to 11%.

This study provided the following conclusions.

• For a constant gas fraction at the pump intake, head degradation decreases as the intake pressure increases.

• Flow conditions become unstable when gas at the pump intake exceeds certain critical limits.

• Mixed-flow, impeller-style pumps handle gaseous fluids better than the radial-stage-style pumps.

• Pump operation was found to be more stable when operating to the right of the best efficiency point.

• Affinity laws could not be applied to the pump under two-phase flow conditions.

No correlations or models were presented by the authors to account for these observations.

Turpin* et al. *(1986).[2] With the data of Lea and Bearden (1982),[1] Turpin developed empirical correlations to predict the head curve for the pumps studied. The factors used to describe head deterioration were the free-gas/liquid ratio, the pump intake pressure, and the intake liquid flow rate. The resulting correlation for I-42B and K-70 pumps is given by

$$H_{TP} = H_{SP} e^{-a_1(q_g/q_l)}, \quad \text{(5)}$$

where H_{TP} = the two-phase flow head calculated with the mixture density, H_{SP} = the single-phase head from the manufacturer catalog, and q_g and q_l are the volumetric flow rates of gas and liquid, respectively, at pump intake conditions. A parameter, a_1, given by

$$a_1 = (346{,}430/p_i^2)(q_g/q_l) - 410/p_i. \quad \text{(6)}$$

For C-72, similar pump correlations are given by

$$H_{TP} = H_{SP} e^{-a_2(q_g/q_l)} [1 - 0.0258\,(q_l - Q_D) + 0.00275(q_l - Q_D)^2 - 0.0001\,(q_l - Q_D)^3], \quad \text{(7)}$$

where a_2 and Q_D are given by

$$a_2 = (285{,}340/p_i^2)(q_g/q_l), \quad \text{(8)}$$

and $Q_D = 98.3 - 33.3\,\phi$, (9)

respectively.

The parameter ϕ is calculated with

$$\phi = 2{,}000\left(\frac{q_g/q_l}{3p_i}\right). \quad \text{(10)}$$

Curiously, pumps I-42B (radial flow) and K-70 (mixed flow) share the same correlation even though they have a different hydraulic design.

The authors also suggested using ϕ as a criterion to check whether the pump can operate under gassy conditions. When ϕ is less than 1, the pump can operate in the presence of free gas, and head correlations can be used to estimate the expected head. When ϕ is greater than 1, the pump is susceptible to significant head degradation, and the head correlations are not suitable.

These correlations were designed for flow higher than the best efficiency point.

Dunbar (1989).[3] The author presented a general correlation in graphical form. Unfortunately, his work does not provide information on theoretical aspects, experimental testing, or the field data used. Accordingly, with Lea and Bearden's[1] earlier observations, Dunbar's approach[3] predicts more stable pump performance at higher pressures for a given gas-liquid ratio.

A very useful aspect of this method is that all stages that are required to develop any pressure with a vapor/liquid ratio of less than Dunbar's factor[3] curve at a given pressure must be corrected to show a reduced amount of pressure based on how far below the curve they operate.

Pump performance can be corrected on the head by obtaining a factor called ALIM from Dunbar's factor curve[3] and another called BLIM that is based on experience. However, no procedural detail was presented to estimate those coefficients.

Cirilo (1998).[4] This author measured the performance of three different submersible centrifugal pumps handling two-phase flow. Two pumps were of mixed flow type with 4,000 and 7,000-barrels-per-day (BPD) best-efficiency flow rate, and another was a radial type with a 2,100-BPD best-efficiency flow rate. Air and water were used as the test fluids. The data were gathered as a function of the gas fraction, pump intake pressure, pump geometry, and speed. The head was calculated with a homogeneous mixture density.

The phenomenon of pump instability as a function of intake conditions was also detected by Cirilo.[4] It was observed that for all three pumps tested, the pump's ability to handle free gas increased as the intake pressure increased. The effect of free gas on pump performance is especially dramatic at low liquid flow rates. Given a certain gas percentage, there is a point at which the pump head increases with an increasing flow rate (positive slope). These points are close to where surging begins, and no additional, stable points can be taken for lower liquid flow rates.

Comparing all three pumps, the mixed type (a 7,000-BPD best-efficiency flow rate) exhibited the lowest deterioration, while the radial pump, with a best-efficiency flow rate of 2,100 BPD, showed the highest.

With respect to the speed effect, Cirilo[4] observed little improvement in the pump's ability to handle gas in tests that increased the frequency from 45 to 65 Hz.

Finally, Cirilo[4] studied the effect of varying the number of stages for the mixed-type pump with a 4,000-BPD best-efficiency flow rate. An example of his results is shown in **Fig. 4,** which indicates a definite trend of less head deterioration with more stages. This result is expected because the later pump stages handle a smaller free-gas fraction, operating at correspondingly lower flow rates and developing higher head.

Fig. 4 is a good example of the dependence of the averaged experimental pump head and the number of stages. Because this figure represents the behavior per stage, it should be independent of the number of stages and, as can be seen, different results are obtained. A correlation developed with the data for six stages will not be useful in predicting pump behavior when 12, 18, or any other number of stages is used.

A simple correlation was given by Cirilo[4] to determine the maximum free-gas fraction (λ_g) for stable operation (surging):

$$\lambda_g = 0.0187\, p_i^{0.4342}. \quad \text{(11)}$$

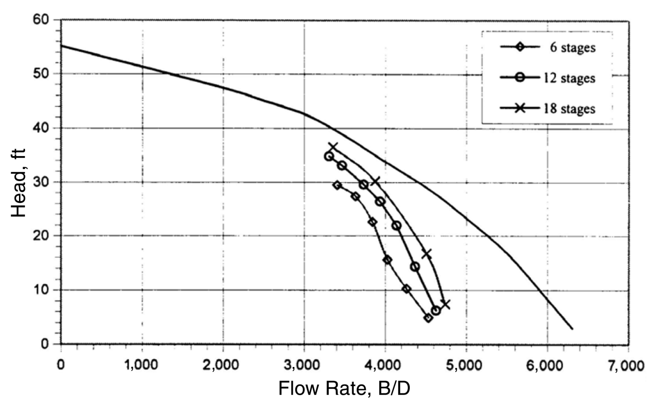

Fig. 4—Performance curve for different number of stages, 15% free gas, and a 200-psig pump intake pressure for a mixed type with BEP=4,000 B/D.

This correlation is limited to the right of the best efficiency point (BEP) for gas void fractions greater than 15% and does not depend on pump speed, number of pump stages, or geometry.

***Pessoa* et al. *(1999).*[5]** These authors performed some tests with a tapered, 20-stage, highly axial flow pump composed of a 104-stage mixed-flow type with a best-efficiency flow rate of 4,100 BPD. Real crude and gas were used as fluids at the experimental well. Both single- and two-phase tests were conducted with light (32.5°API) and heavy (11.6°API) crude oil with a 0.7-s.g. natural gas. The pump intake pressure ranged from 150 to 400 psig.

One main objective of the test was to obtain information on the amount of free gas handled by the ESP system for different operating conditions. For light oil, the maximum free gas by volume, which the tapered pump system handled without pressure fluctuations, was 50%. For heavy oil, the maximum free gas by volume was 42%.

Gas-locking tests were also performed. Before the gas lock occurred, high wellhead and pump-intake pressure fluctuations were observed. Gas lock never occurred with heavy oil.

The authors faced the problem of how to generalize the results in terms of the head developed by stages. They presented their results in the form of a dimensionless pressure difference defined as the relation between two-phase measured Δp and single-phase Δp (manufacturer specifications) for the same liquid flow rate.

Pessoa *et al.*[5] observed a relative increment of approximately 10% in the dimensionless Δp with heavy oil. It was attributed to the apparent viscosity reduction caused by gas presence.

***Romero (1999).*[6]** This author evaluated an improved model of the gas-handling stage with a slotted impeller designed to increase the maximum free-gas fraction ESPs can handle. Cirilo's[4] experimental data for a 12-stage, mixed-type pump with a best-efficiency flow rate of 4,000 BPD established a comparative base scenario without the gas-handling device. The main objectives were to generate enough useful information to characterize the equipment, allowing easier sizing and checking its limitations in the gas-handling task. Some correlations developed for the pump are given by the following expressions.

$$H_d = \left(1 - \frac{q_d}{q_{d\max}}\right)\left[a\left(\frac{q_d}{q_{d\max}}\right)^2 + \frac{q_d}{q_{d\max}} + 1\right], \quad (12)$$

where H_d = two-phase flow dimensionless head per stage and q_d = the dimensionless liquid flow rate defined by Eqs. 13 and 14, respectively.

$$H_d = H_{TP}/H_{SP}^{\max}, \quad (13)$$

$$q_d = q_{TP}/q_{SP}. \quad (14)$$

Here, $H_{SP}^{\max}$ = the shut-in value for single-phase flow (water). For the development of Romero's correlation,[6] both variables (the head and the flow rate in two-phase flow) were calculated at average conditions between the pump inlet and outlet. The resultant total head was then averaged by the number of stages.

The parameters a and $q_{d\max}$ in Eq. 12 are calculated with the following correlations.

$$a = 2.902\,\lambda_g + 0.2751, \quad (15)$$

and $q_{d\max} = 1 - 2.0235\,\lambda_g$. (16)

Eq. 16 represents the dimensionless maximum liquid volumetric flow rate handled by the pump for a certain free-gas fraction.

Another correlation was developed to determine the limiting flow rate under which surging occurs. In a dimensionless form, it is given by

$$q_{d\lim} = -6.6465\,\lambda_g^2 + 3.5775\,\lambda_g + 5.4 \times 10^{-3}. \quad (17)$$

Finally, the author also developed correlations to calculate the maximum free-gas fraction at intake conditions for stably operating each piece of equipment and when operating in tandem. For the pump only, we have

$$\lambda_g = 0.004\,(p_i - 14.7)^{0.6801}. \quad (18)$$

***Sachdeva (1988).*[7]** Sachdeva presented the first comprehensive model for the petroleum industry. Data from Lea and Bearden[1] were used to calibrate the model and develop a correlation for the two-phase flow head.[8]

Sachdeva[7] adapted the nuclear-industry models for multistage pumps used in ESPs. However, the nuclear-industry models cannot be used in the petroleum industry for the following reasons.

- Nuclear-industry pumps are volute-type and single-stage (as opposed to diffuser-type, multistage ESPs).
- Pump diameters are substantially larger (scaling effects are unknown).
- Most models are valid for low inlet free-gas fractions (<10%).
- Most studies have low inlet pressures (<10 psig).
- No pressure (multistage) effects are considered.

The model is 1D and based on the streamline approach. Five fundamental equations were used.

- Two mass balance equations, one for each phase.
- Two momentum equations based on the two-fluid approach instead of the drift-flux approach and concentrated in bubbly flow (although some modifications were introduced later for other flow regimes).
- One equation of state for the gas phase, the thermodynamic behavior of which was assumed to be adiabatic.

The model predicts some observed trends in ESPs but had some drawbacks, mainly related to its complexity and its dependency on an empirical closure relationship.

Conscious of these limitations, in 1992, Sachdeva published a correlation to estimate the pressure difference across each stage under multiphase conditions.[8] It was based on the results of his dynamic model and is given by

$$\Delta p = K(p_i - 14.7)^{E1}\,(\lambda_g)^{E2}\,(q_1)^{E3}. \quad (19)$$

Here, the free-gas fraction is at the intake conditions, and K, $E1$, $E2$, and $E3$ are constants developed by regression analysis from Lea and Bearden's[1] data. Their respective values are shown in **Table 1.**

TABLE 1—SACHDEVA'S[8] CORRELATION PARAMETERS

Pump Model	*K*	*E*1	*E*2	*E*3
I-42B	114.34237	0.943308	−1.175596	−1.300093
C-72	3.9381671	0.875192	−1.764939	−0.918702
K-70	0.2872348	0.622180	−1.350338	−0.317039

Basic Concepts. Through the literature review presented previously, it can be seen that authors use different Nomenclature and even different terminology to refer to the same phenomena.[1–8]

Before comparing these methods, some concepts basic to centrifugal pump behavior analysis under two-phase flow conditions must be defined. These concepts are the head, free gas content, surging, and gas locking.

Head. From its units, the head can be thought of as a parameter that equalizes the energy in a fluid and the pressure developed by a vertical column of that fluid. It can be defined as a parameter conveniently used in fluid mechanics to describe the amount of energy in a fluid per its unit weight. It includes the kinetic, potential, and pressure energy contributions to the total fluid energy.

In centrifugal pumps, the pressure energy is large compared with kinetic and potential energy contributions. For this reason, the pressure-head term defined in Eq. 2 has traditionally been used to quantify the pressure energy delivered by these machines.

For centrifugal pumps handling two-phase mixtures, the pressure-head calculation with Eq. 2 is a problem because of the compressible nature of the fluid. The problem gets worse for multistage centrifugal pumps, such as ESPs, in which the pressure and density are averaged through the number of stages (n). In this case, Eq. 2 becomes

$$H = \Delta p/(ng\rho_{TP}). \quad (20)$$

The two-phase density (ρ_{TP}) in this equation is calculated by most authors according to one of the following methods.[1,2,4,6–8]

• An average mixture density between the stage inlet and outlet conditions.

$$\overline{\rho_{TP}} = (\rho_{TP}^{\text{intake}} + \rho_{TP}^{\text{discharge}})/2. \quad (21)$$

• A mixture density at the average pressure and temperature conditions between the inlet and outlet. Here, the gas and liquid densities are determined at average conditions and used in the following equation.

$$\rho_{TP} = \lambda_g\, \rho_g + (1 - \lambda_g)\, \rho_l. \quad (22)$$

The two-phase head calculated with any of these density variants is not constant for the same pump as described for single-phase flow. Furthermore, because the head is calculated as an average per stage and because the density depends on the delivered pressure (that is, a function of the number of stages), the head becomes a function of the number of stages in the pump.

Free-Gas Content. Usually, free gas handled by the pump is calculated as a volumetric fraction of the total phases present and referred to as the pump intake conditions.

In the experimental studies presented previously,[1,4,6] the volumetric relationships used by the authors were the nonslip free-gas fraction (also known as the nonslip gas-void fraction) and the free-gas/liquid ratio or vapor/liquid ratio.

Some authors[4,6–8] refer to the gas fraction with the Greek letter α. Traditionally, this notation refers to the slip gas-void fraction, not to the nonslip gas-void fraction, which is denoted by λ_g. In an attempt to standardize the Nomenclature, this work delineates the difference between slip and nonslip gas-void fractions. A few works, such as the one by Furuya,[9] have considered the slippage between phases.

The free-gas/liquid ratio (R_F) parameter is defined as the free-gas flow rate (q_g) divided by the liquid flow rate (q_l), both at in-situ conditions.

$$R_F = q_g/q_l. \quad (23)$$

The free-gas fraction or nonslip gas-void fraction is the free gas flow rate divided by the total flow rate.

$$\lambda_g = q_g/(q_g + q_l). \quad (24)$$

With these equations, a relationship between the free-gas/liquid ratio and the free-gas fraction can be established as

$$R_F = \lambda_g/(1 - \lambda_g). \quad (25)$$

Surging. Another important definition that must be introduced is the surging observed and mentioned in all ESP studies concerning two-phase flow conditions.

Surging is a cyclic fluctuation of the system's pressure. It is also known in the literature as "heading." "Pressure instability" is also used in reference to this phenomenon.

Some centrifugal pumps present a particular head-capacity behavior prone to pressure instability with single-phase (liquid) flow. This undesirable behavior is characterized by a region with a positive slope for the head performance curve.

Surging is a system phenomenon, not just a pump phenomenon. However, pump head vs. capacity can influence the occurrence or the severity of the problem.

Surging has not been documented as a particular topic for pumps under two-phase flow, so the phenomenon that takes place within the pump is not well understood. Many investigators, however, have studied this condition for single-phase flow. In some experimental studies[10] available from the nuclear industry, surging appears as a discontinuity in the head performance, which is a consequence of a change in the flow pattern. The author of these studies pointed out that reverse flow occurs during this stage.

Gas Locking. Another important concept useful when dealing with centrifugal pumps that handle two-phase mixtures is the gas-lock condition. When a pump reaches this state, the pumping action just stops, leaving it virtually unable to deliver any head.

The gas locking that occurs in ESPs is similar to the loss of prime condition. This terminology is used more commonly by manufacturers of surface centrifugal pumps that use one or very few stages.

The difference between gas locking and gas blocking[11] also must be understood. During gas blocking, the pump keeps developing some head and pumping fluids but with a lower capacity than before the condition was reached. This is caused by gas accumulation in the low pressure side of the impeller vanes. The static gas pockets interfere with the flow by partially blocking the flow area.

Comparison of Previous Works. This section analyzes experimental studies by establishing their limitations and comparing them under the same standards.

These studies have treated the ESP as a black box, measuring some thermodynamic properties only at intake and discharge points and masking the behavior stage by stage. **Fig. 5** shows this limitation.

The correlations developed for two-phase flow on the basis of the average results per stage are pump-specific.

Pump Performance Prediction. Because the fundamental objective of pumps is pressure increment, authors show more concern with head degradation than other performance parameters.[1–8]

Two-phase head correlations are available only from Turpin[2] and Romero's[6] works. These correlations were developed for data matching, not as predictive tools to estimate the performance of other pumps.

Turpin and Romero[2,6] differ greatly in the assumptions considered in developing their correlations. Turpin[2] assumed that the head delivered by ESP stages is a function of the pump intake pressure. Romero,[6] on the other hand, believed that the difference in terms of pump-generated head is very small for different intake pressures and constant free-gas fraction. Therefore, she neglected these differences in her correlation development.

Both authors used the liquid volumetric flow rate instead of the total mixture flow rate. A comparison between theirs and the traditional methods presented previously is shown in **Fig. 6** as it applies to the mixed-type pump with a best-efficiency flow rate of 6,100 B/D. A pump intake pressure of 100 psig and a free-gas percentage of 20% were assumed at 60 Hz.

Sachdeva's dynamic model[7] to predict pressure behavior per stage is not easily comparable with the empirical correlations because he predicts pressure instead of head. The curves in **Fig. 7,** however, were plotted with Eq. 19 and based on the results of his dynamic model for a pressure of 200 psig and different free-gas fractions.

Unfortunately, possibly because of a problem related with the narrow data range in which the correlation was developed, its shape does not match that of the experimental curves. Because of the negative sign in parameters *E*2 and *E*3 in Table 1, Sachdeva's correlation acquires a hyperbolic form (upward concavity), which is completely different from the downward concave of typical head curves. Obviously, its extrapolation outside the data range will result in incorrect predictions.

Free-Gas Content. All studies reviewed coincide in quantifying the gas based on volumetric variables. Lea and Bearden[1] used the free-gas percentage or fraction defined by Eq. 24 to present and group their results. Romero,[6] Cirilo,[4] and Sachdeva[7] chose the same parameter in their works. Turpin[2] used the free-gas/liquid ratio, as defined by Eq. 23, to develop his correlations. Dunbar[3] also selected the free-gas/liquid ratio to present his graphical correlation, even when he called it the vapor/liquid ratio. As demonstrated in the previous sections, Eqs. 23 and 24 can be related through Eq. 25.

Most authors[4,6–8] use the term "void fraction" to refer to the nonslip free-gas fraction, which can be confusing as discussed in the previous concepts section. Furthermore, they use the notation α instead of λ_g, which traditionally has been used to designate the slip gas-void fraction.

Surging Prediction. Based on the observations of Lea and Bearden[1] and later by Cirilo,[4] the surging condition seems to be a function of four variables—the free-gas fraction, the pump intake pressure, and the pump's liquid flow rate and geometry (hydraulic design or type). Therefore, any attempt to define a general corre-

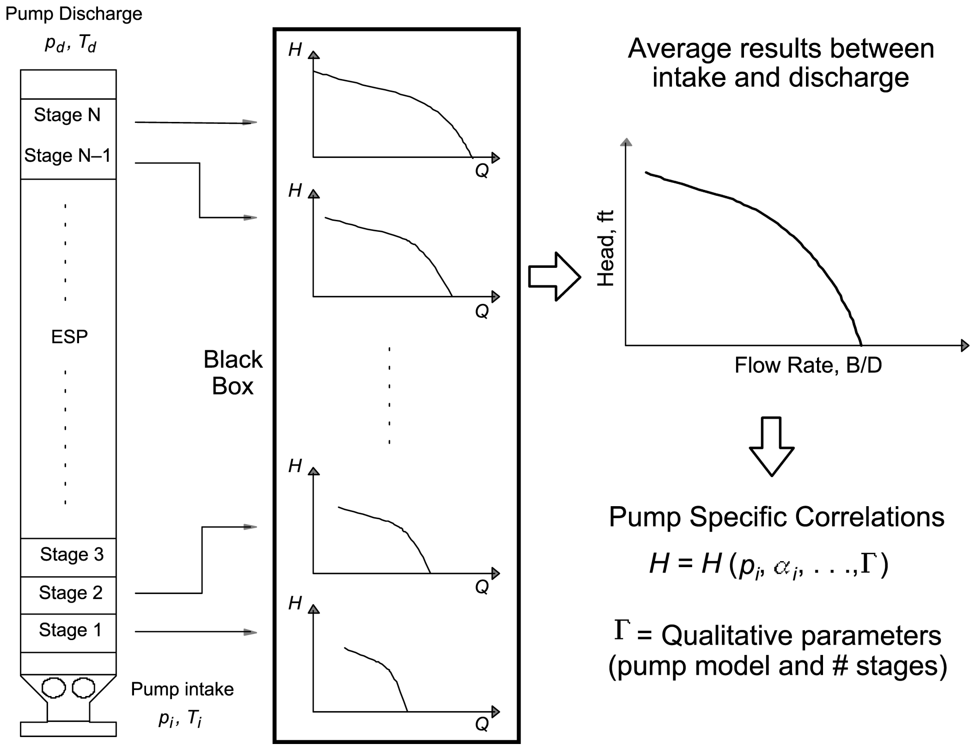

Fig. 5—Specific character of correlations developed in earlier experimental studies.

lation to bound the surging region should establish a functional relationship among these four variables.

Published correlations for surging or pump instability estimation are available from Turpin,[2] Dunbar,[3] Cirilo,[4] and Romero.[6] A comparison of their results is shown in **Fig. 8.** These correlations basically establish a surging relationship as a function of the free-gas fraction and pump intake pressure. They do not include either other variable or the experimental system effect.

As observed in this figure, Turpin's correlation,[2] expressed by Eq. 10, represents the more optimistic scenario. The dashed line means that the curve was extrapolated beyond the experimental range of correlation development.

The Dunbar factor curve[3] represents the more conservative limit if considered as a surging boundary up to 550 psia.

Cirilo's correlation[4] predicts free-gas fractions of more than 1 when the pump intake pressure is greater than 9,552 psia. The surging boundary introduced is between Turpin and Dunbar's curves, up to approximately 550 psia.[2,3]

Romero's correlation,[6] given by Eq. 18, is similar in shape and variables to other authors' predictions. It has the same drawback as Cirilo's correlation,[4] predicting free-gas fractions of more than 1 but for pressures of greater than 3,371 psia in this case. Her correlation, given by Eq. 17, is the only one that involves the liquid flow rate and is used to predict the minimum flow rate for different free-gas fractions before surging appears.

Gas Locking Prediction. In the literature,[1–10,12] none of the authors presented data or correlations to predict the gas-lock condition. This phenomenon seems to appear after surging, an undesirable condition.

Pump and Facility Modifications and Data-Acquisition System Development

The experimental tests were conducted at the TUALP two-phase-flow ESP test facility used by Cirilo and Romero.[4,6] Modifications were performed to accommodate the 22-stage, mixed-flow-type ESP (with a best-efficiency flow rate of 6,100 B/D) and to improve the accuracy and acquisition of the data. The pump was also modified to allow the pressure sensors to connect and communicate with the fluid path. The modifications performed can be grouped in four categories.

- Pump modification.
- Upgrade of instrumentation.

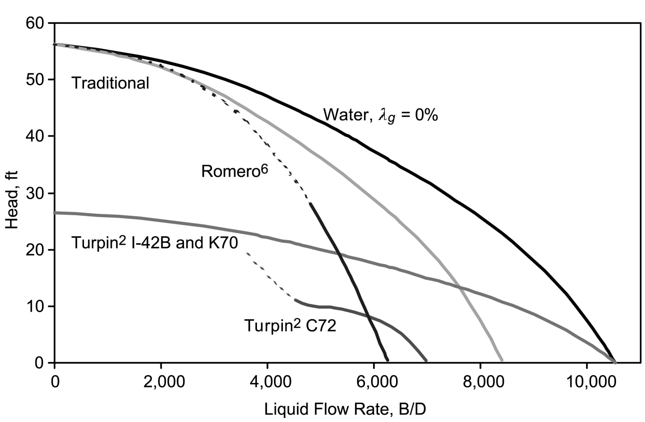

Fig. 6—Head prediction comparison by Romero, Turpin, and traditional methods applied to the mixed type pump with BEP=6,100 B/D.

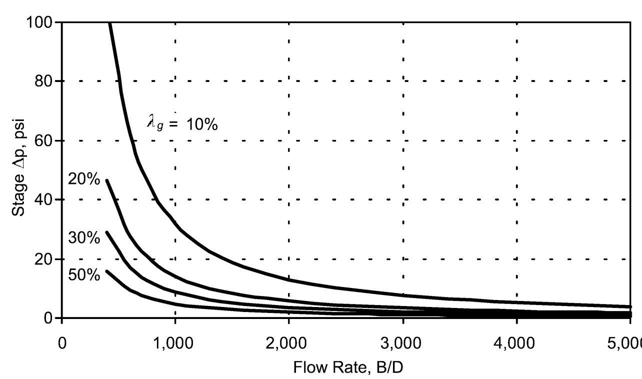

Fig. 7—Sachdeva's correlation shape for a pump intake pressure of 200 psig.

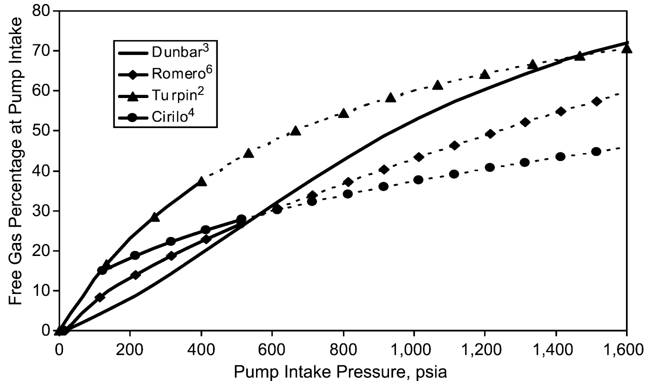

Fig. 8—Comparison of available empirical correlations for stable pump operation.

Fig. 9—Diffuser stage of pump (tested).

- Mechanical modifications of facility.
- Development of a data-acquisition and control system.

Pump Modification. Two possible ways were considered to mount the sensors on the housing—directly threaded or welded taps. During the welding process, the housing is heated, which could cause bending, or a snake effect. For this reason, the preferred choice was to thread the ports directly to the pump. Because of limitations imposed by the housing thickness (~0.33 in.), this alternative required a sensor connector with a shallow thread. To overcome this problem, a 22-stage, mixed-type pump was selected that presents a groove or channel around the diffuser end of the stage, allowing a deeper penetration of the sensor connector, as can be seen in **Fig. 9.**

To avoid installation interference among the pressure transmitters, 3/8-in. holes were drilled on the housing with their locations alternating by 90 degrees. **Fig. 10** shows an axial section of the pump through one of the two drilling planes.

To facilitate communication between the pressure sensor and the pumped fluid, two 1/8-in. holes were drilled diametrically opposite each other on each diffuser. The holes were drilled near the stage end (vanes region) and in the middle of the channel bounded by two consecutive vanes because these were assumed to be representative of the average conditions in the diffuser channels. The stage diffuser hole can be seen in Fig. 9.

Because holes were drilled on each diffuser, a seal (obtained with o-rings on all diffusers) was required to isolate the stages. An annular space was created this way between two consecutive diffusers, their o-rings, and the pump housing. When the pump was operating, this annular area self-filled with the pumped mixture.

Instrumentation Upgrade. The main purpose of this study was to measure the pressure in a considerable number of ESP stages under two-phase flow conditions. An efficient way to record all the information simultaneously was required.

For this reason, pressure and temperature electronic transmitters were used instead of manometers and local temperature indicators. Similar reasoning was applied to the flowmeters installed, which were replaced by Micro Motions.*

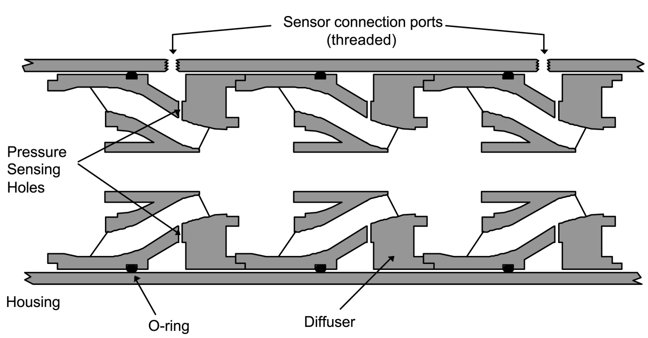

Fig. 10—Axial section of the pump through one of the sensor holes planes.

Because of budget limitations, a total of 17 pressure sensors were acquired instead of the 24 required to fully instrument the pump (22 stages plus pump intake and discharge). The final distribution of these 17 sensors is shown in **Fig. 11.** Special attention was given to the first 10 stages, where the free gas has the highest effect.

To improve the resolution of the sensors scale, it was calibrated along the ESP in accordance with the progressive pressure increment.

For liquid and gas flow-rate measurement, Coriolis mass flowmeters were acquired.

These instruments were selected based on their accuracy, environmental work conditions, and operating range. The calibration span was adjusted to improve the resolution of the sensed variable.

Mechanical Facility Modifications. The TUALP existing facility was modified to accommodate the pump and the instruments acquired. The liquid sensor used to determine water mass flow rate was placed in the liquid line between the booster pump and the ESP. At that location, the injected water should be free of vapor bubbles. A picture of the test bench after the modifications is shown in **Fig. 12.**

Development of a Data-Acquisition and Control System. A computer-based data-acquisition system (DAS) is the most efficient way to collect all the information simultaneously.

The hardware used to build this application required special modules for conditioning the signals, and an appropriate module was selected depending on the signal type. These modules were mounted on a chassis, and a computer was used to retrieve, monitor, and store the required variables with adequate software. A data-acquisition card was inserted into the computer and worked as the interface between the computer and the chassis. A personal computer was used to run the DAS.

A friendly graphical interface was developed with LabVIEW.** It made controlling the ESP pump and monitoring and storing variables through the computer easier.

Facilities Description

A simplified diagram of the two-phase flow facility and ESP test bench used in this work are presented in Fig. 11.

The liquid phase (in this case, water) is stored in a 500-barrel tank. It worked as a liquid reservoir feeding a centrifugal booster pump. Two manual valves, PCV-1 and PCV-2, were used to control the liquid pressure by recirculation through bypass lines.

* Micro Motion is trademarked to Micro Motion Inc., Boulder, Colorado.
** LabVIEW is a trademark of Natl. Instruments Corp., Austin, Texas.

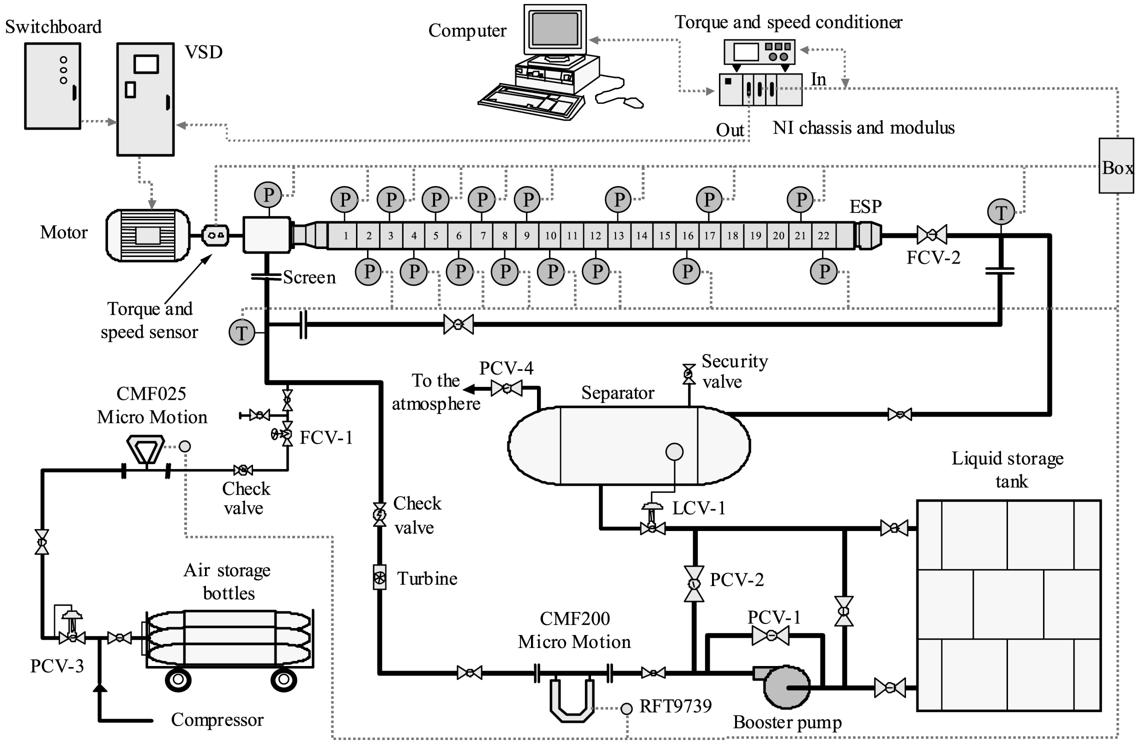

Fig. 11—Scheme of the TUALP ESP experimental facilities.

The pressurized liquid was conducted to the flowmeter through a 3-in. pipe.

The gas phase (in this case, air) was stored in high-pressure cylinders, up to 1,500 psig. A compressor was used to charge the cylindrical bottles. The PCV-3 valve worked as a pressure regulator, reducing and keeping it constant.

After the pressure regulator, the air travels a distance of approximately 250 ft through a 3-in. line until reaching the gas flowmeter. Downstream of it, ½-in. stainless steel tubing was used to conduct the air to a needle valve (FCV-1) for injected air flow-rate control.

The gas and liquid pipelines merged approximately 7 ft from the pump intake.

A screen with ¼-in. holes was installed 10 in. upstream of the pump-intake chamber to promote gas-liquid mixing, even though Cirilo[4] experimentally demonstrated that changing the diameter of the screen holes had no influence on pump performance.

The ESP test bench is a steel structure that accommodates the submersible pump in a horizontal position. The pump was driven by a 40-hp motor, controlled by a variable speed drive (VSD). Remote control was implemented through the VSD.

A combination of torque and speed sensors was coupled between the motor and the submersible centrifugal pump. They sensed the shaft torque and angular speed, respectively.

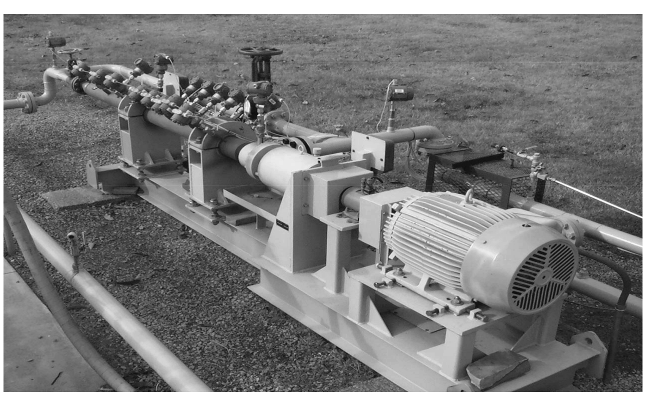

Fig. 12—ESP test bench after modifications.

The gas-liquid mixture arrived in a thrust chamber capable of handling pressures up to 1,000 psig. It seals the shaft, avoiding fluid leaks, and works as the intake section of the submersible pump. The first pressure sensor is located immediately above this chamber.

A manual-valve globe (FCV-2), installed downstream of the ESP, was used to apply backpressure to control the flow through the pump. The exhaust fluid (either liquid or a mixture of gas and liquid, depending on the tests) was sent to a horizontal separator, then back to the storage tank through the level control valve LCV-1, while the gas was vented to the atmosphere through Control Valve PCV-4.

The pipelines in this loop are not thermally insulated.

Experimental Matrix

The fluids selected for this study were fresh water as the liquid phase and air as the gas phase. A mixture of these components has the following important advantages.

- The amount of air dissolved in water is negligible, so all the air injected can be considered free gas.
- The physical properties are well known.
- It is environmentally friendly.
- It has low security risks.
- The cost of water and air is minimal with respect to any other fluids.

Before running air-water experiments, single-phase (water) tests were initially considered for this study. Their objectives were to check for a good seal between stages, to compare pump performance with the manufacturer catalog curves, and to establish the maximum delivered pressure for each stage.

For the water tests, two pump intakes were analyzed—20 and 250 psig. The experimental matrix was designed with a varying liquid flow rate to cover the range from the maximum allowed by the flow loop (FCV-2 full open) to 0 B/D in steps of approximately 600 B/D for both pump-intake pressures.

Because these tests were done with 100% liquid, affinity laws could be used.

Defining the tests to be carried out in two-phase flow was a more difficult task. In earlier experimental studies,[1,4,6] researchers kept the pump-intake pressure and free-gas volume fraction constant. In this study, an experimental matrix based on changing only one flow rate at a time was adopted to make the experiments easier.

The problem with designing an experimental matrix under these assumptions arises from the uncertainty of each variable's unknown limits. The maximum liquid flow rate the pump can handle changes for each injected gas flow rate. The minimum liquid flow rate also depends on the injected amount of gas and must correspond to a surging or near-gas-lock condition.

Considering all these limitations, the experimental matrix was proposed with a variable step for the liquid and gas flow rates instead of a constant step. A minimum of eight points was measured for each gas flow rate and pump intake pressure between the gas-lock condition and the maximum liquid flow rate.

Because of time limitations, tests varying the spin direction, pump intake pressure, and angular speed were not possible.

In summary, the air-water tests were done at a constant angular speed of 3,208 rpm (55 Hz) and a clockwise spin direction (discharge view) within the following ranges.

- Pump intake pressure = 100 psig.
- Liquid flow rate = 900 to 8,200 B/D.
- Gas flow rate = 5,000 to 39,000 scf/D.

Test Procedure

Three steps common to all experiments were consistently accomplished every day before running the tests. They included warming up the instruments for 30 minutes, building up pressure to drive the pneumatic control valves, and checking the status of manual control valves.

Once these steps were completed, the booster pump was started manually from its switchboard followed by the ESP, started from the data-acquisition and control system. The running frequency was fixed at this point for the ESP via the remote control system.

Water Tests. Once the pumps were running, some time was required to stabilize the separator pressure.

The pressure sensors were bleeding off through a special plug located in the manifold valve for this purpose.

The next step was regulating the ESP intake pressure through Control Valves PCV-1 and PCV-2. Depending on the required pressure, Valve PCV-1 was left completely open (for 20 psig) or closed (for 250 psig), and control was executed with PCV-2 shown in Fig. 11.

Manually adjusting Valve PCV-2 to control the pump intake pressure and FCV-2 to control the liquid flow rate handled was a trial-and-error procedure, requiring multiple steps while the intake pressure achieved for each step was monitored from the control room.

When the pump-intake pressure and the liquid flow rate met the requirements and all conditions held stable for at least 10 minutes, the data were saved to a file for statistical analysis. The information was stored in 1-minute files with a sampling rate of two records per second.

The tests were carried out from the maximum to zero flow rate. The rpm were kept constant because they tend to increase as the liquid flow rate was decreased for each test.

Air-Water Tests. A similar procedure to that for liquid-only tests was followed for the air-water tests. In this case, the gas injection rate was set through the needle, Valve FCV-1 (Fig. 11). The air pressure upstream of this valve was set at 400 psig through Pneumatic Valve PCV-3.

These tests were carried out by keeping the pump intake pressure constant and increasing the rpm and the gas flow rate in steps of 2,500 scf/D. For each gas flow-rate step, the liquid flow rate was varied from the maximum delivered by the pump to the minimum achieved just before the gas-locking condition.

A trial-and-error procedure was followed to get the expected conditions by positioning the PCV-2 valve and the two-phase throttling valve, FCV-2, simultaneously.

The same criterion of stable conditions for a period of at least 10 minutes was used before sending data to a file. As the liquid flow rate decreased for each test, high instability was found for the pump-intake pressure and the liquid flow rate. The rpm increased considerably for these higher free-gas/liquid ratio points, so the pertinent adjustments were made to keep them constant throughout the experimental liquid range.

Similar to the water tests, data were stored in files of 1 minute at a rate of two samples per second.

Experimental Data Analysis

Single-Phase Tests. Single-phase characterization of centrifugal pumps is a must in experimental studies. It sets the base case for performance comparison with two-phase experimental results and allows matching with the manufacturer's catalog specifications to certify that the tested pump meets API standards 11S2[13] for ESP testing. It is also useful to establish whether the instruments used in the loop are calibrated and working properly.

Particular to this study, the single-phase tests were allowed to verify a good seal from stage to stage. Any communication from one stage to another is more likely at the maximum pressure difference that occurs when the ESP is handling 100% liquid and the discharge valve is fully closed (flow rate equal to 0 B/D).

The head performance was calculated per stage with Eq. 2. It was also calculated as an average for the pump by dividing by the number of stages. The water density required in this equation was assumed to be equal to that of fresh water and was corrected by the average temperature across the stage or the pump. A linear gradient was assumed between the pump intake and discharge temperatures.

The density recorded from the Micro Motion flowmeter was not used because it could be influenced by solid particles (mostly rust) present in the water. Additionally, the temperature and pressure at the pump intake and along it were different from those with the Micro Motion.

The average overall brake horsepower (B_{HP}) was computed with Eq. 26. No losses were assumed in the mechanical seal located at the pump intake chamber, so the power consumption was attributed totally to the pump stages.

$$B_{HP} = \frac{\omega\Gamma}{63{,}025.36n}. \quad (26)$$

The efficiency of the pump stages was determined with Eq. 27.

$$\varepsilon = 100\,\frac{q_w H}{135{,}771.43 B_{HP}}\,\frac{\rho_w}{\rho_w^{SC}}, \quad (27)$$

in which q_w and ρ_w are computed at average conditions between pump intake and discharge.

The experimental average head and brake-horsepower results are shown in **Fig. 13** for a pump-intake pressure of 250 psig. It can be concluded from this figure that the pump met API requirements. However, both curves are close to the lower API limit. Because the pump was assembled with some used stages, this could be an anticipated effect.

The average pump's dimensionless head performance per stage is shown in **Fig. 14.** They are compared with the average performance that would be reported by investigators measuring only intake and discharge conditions, as done in the past.

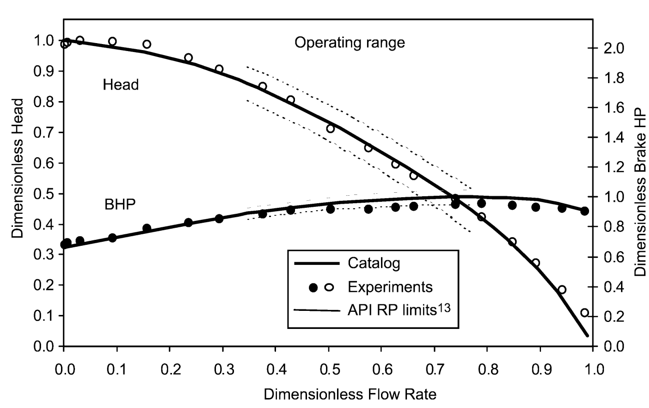

Fig. 13—Comparison between experimental results and catalog specifications for water with pump intake pressure of ~250 psig.

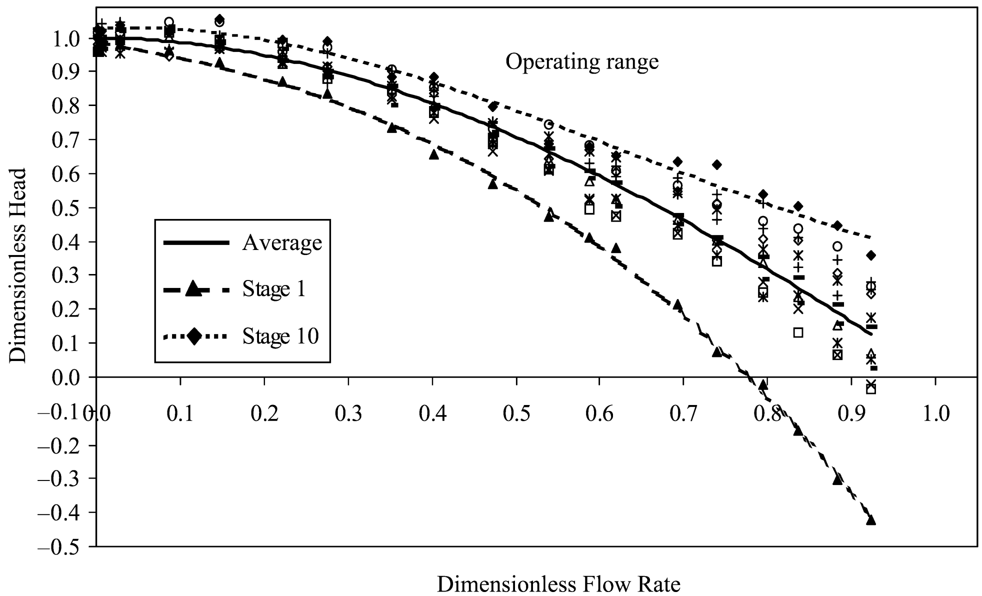

Fig. 14—Comparison between head performance per stage and the pump average for water with pump intake pressure of ~250 psig.

It can be seen from Fig. 14 that each stage has a different behavior. Particularly noticeable is the behavior corresponding to Stage 1, the head performance of which is far lower than the pump average. It did not develop any head after a dimensionless flow rate of approximately 0.78. This bad performance could be caused by an intake effect or because the stage used in the pump assembly is old and exhibits high wear.

Because each stage showed a different head performance, their head curves were made dimensionless to check if they reduced to the same curve. For each stage, the head points were divided by the stage head at a flow rate equal to 0 B/D. The flow-rate points were divided by the maximum flow rate (head = 0 ft) for each respective stage. For those cases in which no zero head was achieved, the maximum flow rate was determined by extrapolating the curve.

The stage-wise dimensionless-head performance curves are shown in **Fig. 15.** It can be seen how the points describe basically the same curve, which was expected because all stages have the same type and geometry.

As mentioned previously, the water tests were also useful in checking for a good seal from stage to stage. For this purpose, the pressure difference delivered per stage at 55 Hz was plotted at a flow rate equal to 14 B/D (minimum available close to 0 B/D). The results are shown in **Fig. 16,** which includes medium and high flow rates for comparison.

For the minimum flow rate of 14 B/D, the pressure difference developed per stage is practically constant, so it can be concluded that the seal between stages was good.

With the higher flow-rate curves in Fig. 16, it is possible to look for low performance stages used in the pump assembly. They are probably old and present some wear. This is the case with Stages 1, 5, 8, and 13, among others.

Two-Phase Tests. The presentation of the results for two-phase flow is a challenge in all experimental studies because of the numerous possible variable combinations. To simplify this task, the graphs presented in this section are mainly a function of the fundamental variables of the liquid and gas flow rates.

The pressure increment in this study was chosen to present the pressure performance of the ESP instead of the head defined by

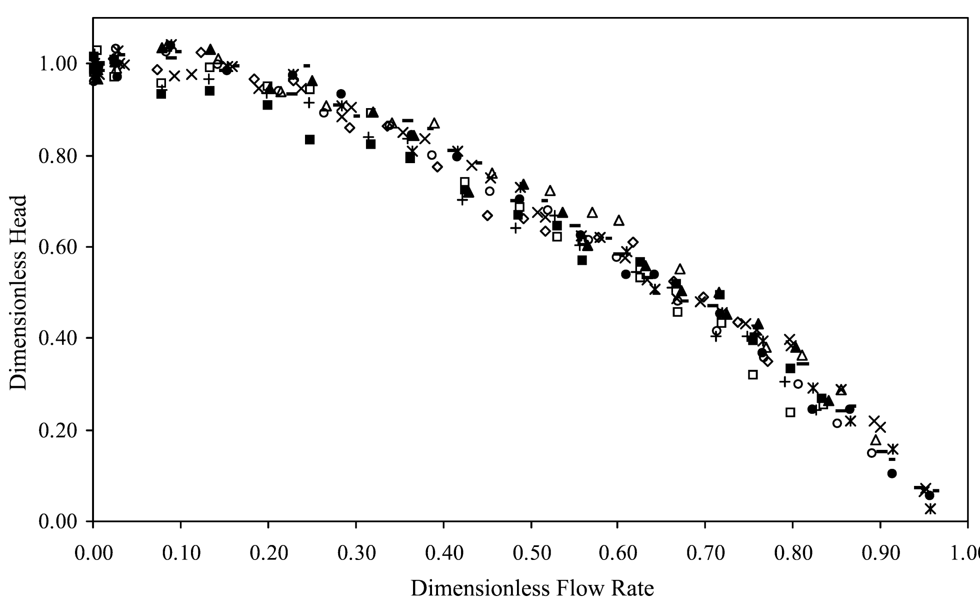

Fig. 15—Dimensionless head performance curves per stage for water tests.

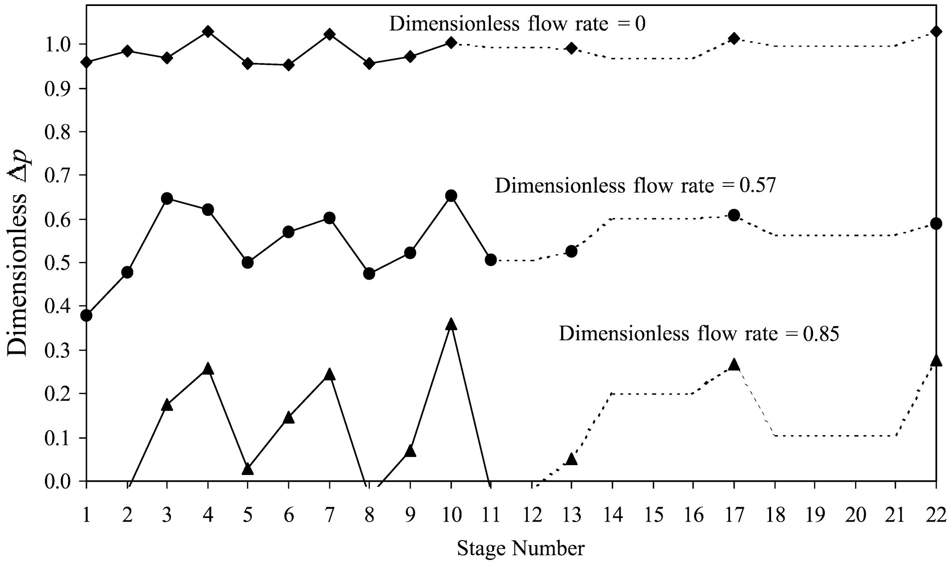

Fig. 16—Pressure difference per stage at different flow rates.

Eq. 20. One of the major limitations to implement this equation is the calculation of a representative mixture density, as discussed previously.

The pressure increment delivered by the whole pump is shown in **Fig. 17** for gas flow rates between 5 and 35 Mscf/D. The single-phase curve (0 scf/D of gas) is included for reference. This figure gives a graphical idea of the experimental window that was covered. The smoothness of the lines can be taken as a visual index of the data quality.

Curiously, at the left of the surging line (dashed line), a minimum in the curves appears for the higher gas flow rates before gas locking is reached. The pressure performance presents a sharp decrease between surging and this minimum. To the left of the minimum, the curves change their slope from positive to negative again, and less fluctuation in pressure and torque were observed in comparison with the surging surroundings. In this region, the pressure delivered is a small fraction of the pump capacity.

Similar curves were plotted per stage. The lines are not as smooth as the average ones for the pump, but the tendency for pressure degradation as the gas flow rate increases is the same.

The first stage lost its pumping capacity for gas flow rates higher than 12.5 Mscf/D, as can be seen in **Fig 18a.** For gas flow rates greater than this value and in the range of high liquid flow rates, it creates a pressure drop at the pump intake.

Because each curve in a plot has a constant gas flow rate, the free-gas fraction increases as the liquid flow rate decreases. The first-stage pressure increment becomes positive at higher free-gas fractions while staying negative at the lower ones.

This strange situation requires further investigation to determine whether the pressure drop occurs in the pump suction (before the stage impeller is reached) or in the first stage. In the latter case, the first stage would only be promoting mixing the liquid and gas phases.

The second and later stages, shown in Figs. 18b through 18d, exhibit a better performance than the first. This can be observed by comparing the wider range of liquid flow rates at which the pressure increment is positive and higher. As the stage intake pressure increases along the pump because of fluids compression, the surging points (absolute maximums) move upward and to the left. This means that the curves become closer to the water curve because of the free-gas-fraction reduction.

To compare the stages' behavior, the pressure increments for all were plotted for each gas flow rate. Type results are shown in **Figs. 19a through 19c.**

A dashed, thicker line in Fig. 19 corresponds to the pump average and would be the resultant line reported if the pressure had been measured only at pump intake and discharge, as done in earlier studies.[1,4,6]

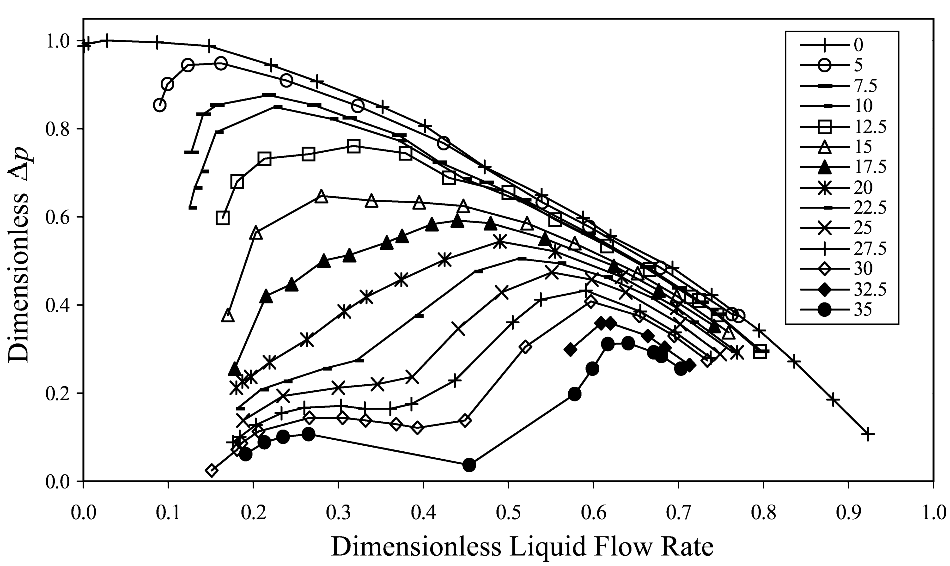

Fig. 17—ESP pressure increment as a function of gas and liquid flow rates.

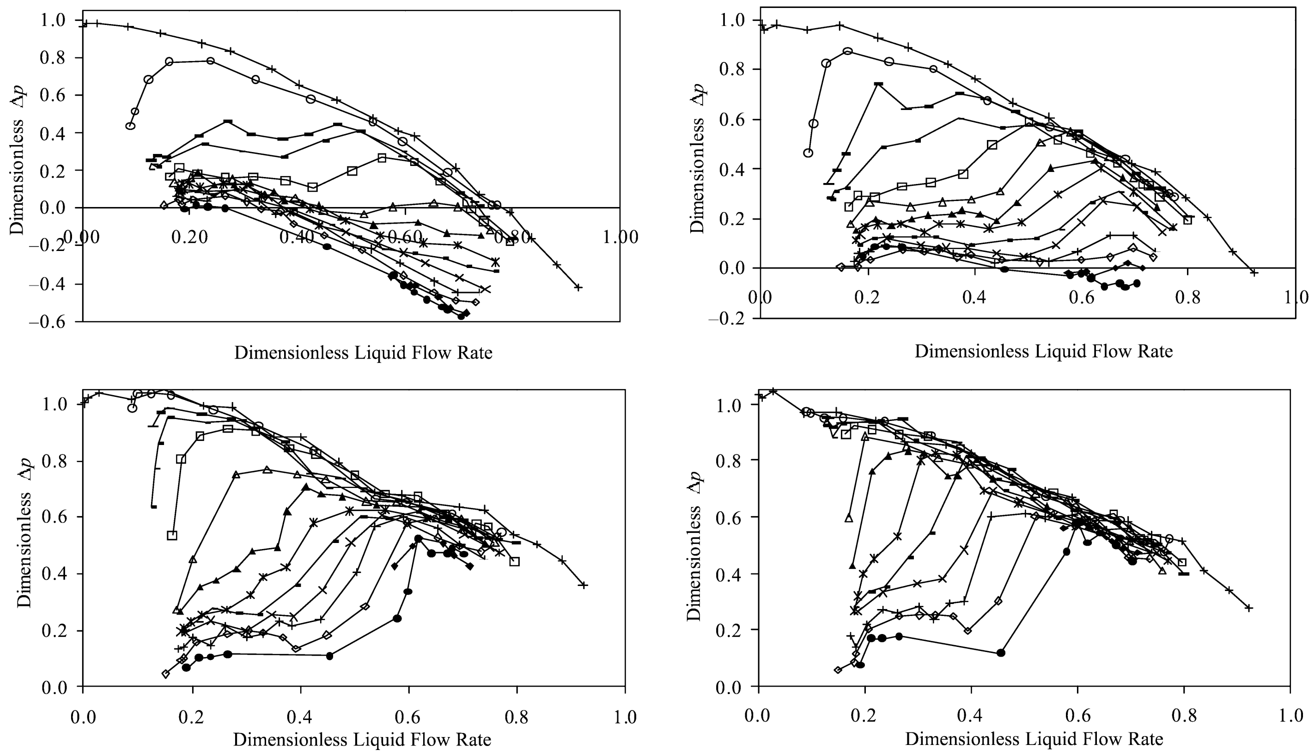

Fig. 18—Pressure increment for Stages 1 (a. upper left), 2 (b. upper right), 10 (c. lower left), and 22 (d. lower right) at different gas flow rates.

For 5 Mscf/D, the pressure behavior per stage is similar to the average for the pump until surging occurs. The curves are close except for the first stage, which shows a significant difference. After surging points for this gas flow rate are reached, the pressure increment decreases until gas lock occurs.

For the next gas flow rate (7.5 Mscf/D), shown in Fig. 19b, the tendency changes, and a depression or valley appears between the surging and the gas-lock points for Stages 1 and 2. The surging point for Stage 3 moved to a higher liquid flow rate (to the right), while it remained practically unaltered for all other stages. As the gas flow rate increased, the same phenomena extended progressively to all other stages.

In a 3D plot, the pressure increment for the pump or the stages can be plotted as a function of the gas and liquid flow rates simultaneously. The result for the pump is shown in **Fig. 20.** The dashed line in the top of the surface represents the surging condition.

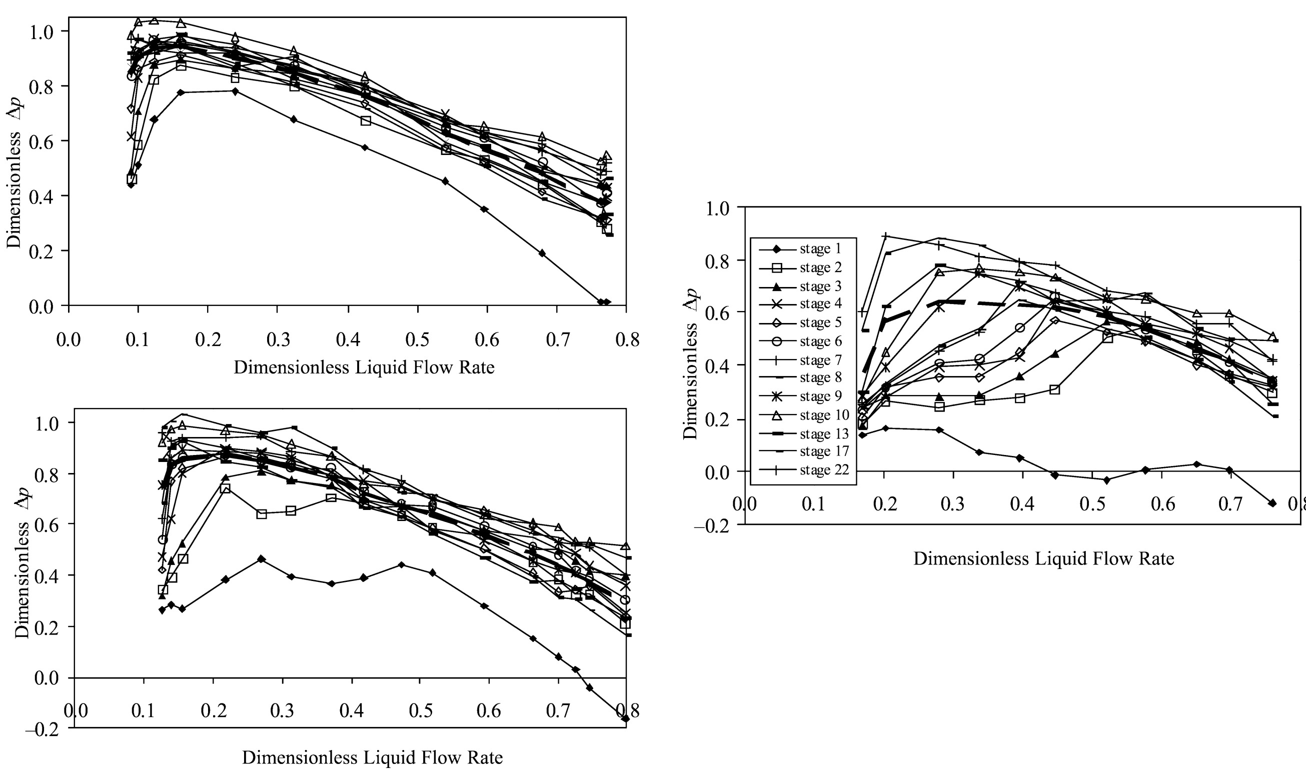

Fig. 19—Pressure increment for all stages at 5 Mscf/D (a. upper left), 7.5 Mscf/D (b. lower left), and 15 Mscf/D (c. right).

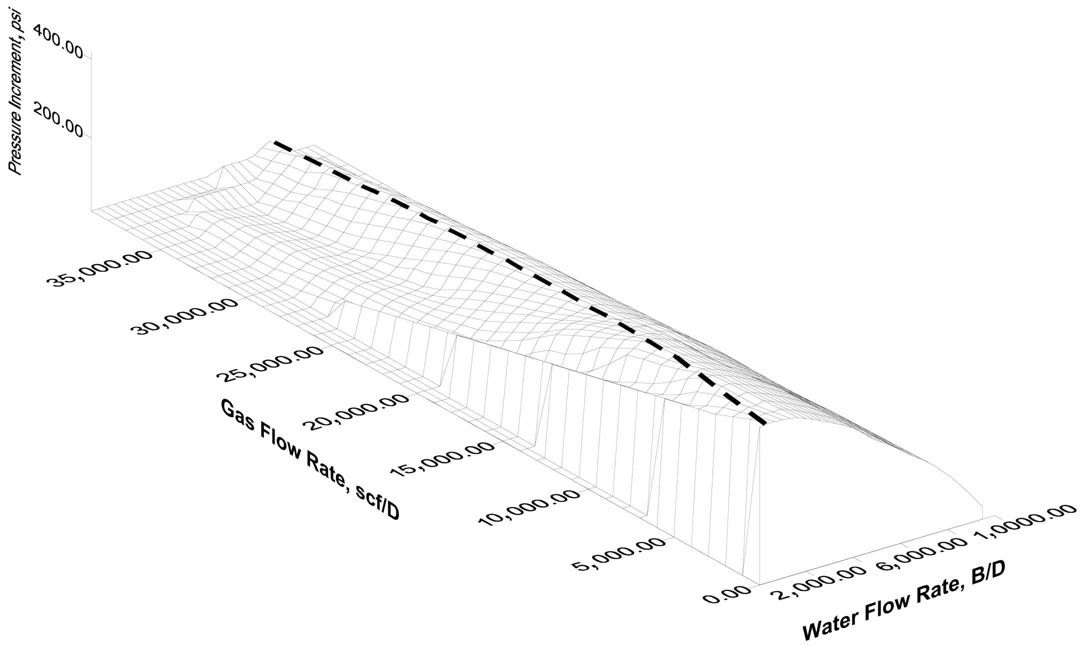

Fig. 20—ESP pressure increment as a function of gas liquid flow rate—3D view.

An aerial view of this plot is shown in **Fig. 21.** A plot of the free-gas fraction at the pump intake has been superimposed in Fig. 21b.

In this study, the hydraulic horsepower delivered to the fluid was calculated as the sum of the water and gas contributions. For water, the following equation was used.

$$Hp_w = \frac{144}{60 \times 550} \Delta px \frac{\dot{m}_w}{\rho_w}. \quad (28)$$

Here, the pressure increment is for each stage. The density was calculated at the average temperature between each stage's intake and discharge, assuming a linear temperature gradient between the pump intake and its discharge.

For the gas phase, the calculations were made assuming two possible behaviors—isothermal and adiabatic, as described by Eqs. 29 and 30, respectively.

$$Hp_g^{\text{isoth}} = \frac{144}{60 \times 50} \frac{\dot{m}_g RT}{M_g} \ln\left(\frac{p_1}{p_2}\right), \quad (29)$$

and

$$Hp_g^{\text{adb}} = \frac{144}{60 \times 550} \frac{\left(\frac{p_2}{p_1}\right)^{\frac{1-k}{k}} - 1}{1-k} \left(\frac{\dot{m}_g RT_1}{M_g}\right). \quad (30)$$

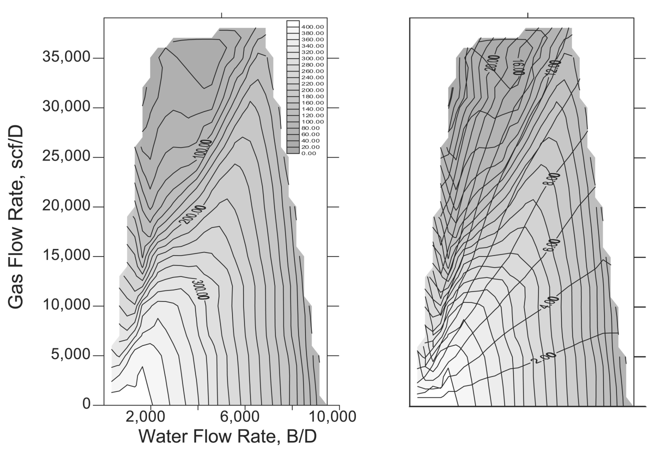

Fig. 21—ESP pressure increment behavior—gas and liquid flow rates and free-gas fraction effect.

The isothermal process delivers higher amounts of energy to the fluid than the adiabatic process. As the gas flow rate increases, it is possible to see how the horsepower wasted to compress the gas becomes an important factor when compared with the one for water. This is more critical at low liquid flow rates, at which the free-gas fraction turns higher. An example is given for Stage 3 in **Fig. 22.**

The average total hydraulic horsepower curve for the pump with each gas flow rate is shown in **Fig. 23.** The information is also available per stage as shown in **Fig. 24.** In general, the hydraulic horsepower delivered to the fluids decreases as the gas flow rate increases. On the other hand, it increases from stage to stage as the mixture passes through the pump. These plots also verified the mixing labor of the first stage, which degrades faster than the others.

The brake horsepower for these tests was measured for the total pump only because it is difficult to measure stage by stage. A plot of the resultant performance for each gas flow rate is shown in **Fig. 25.**

Based on the total hydraulic and the brake horsepower measured for the pump, average efficiency curves were developed for each gas flow rate. The following expression was used.

$$\varepsilon = 100 \frac{Hp_g + Hp_l}{B_{HP}}. \quad (31)$$

The results are shown in **Fig. 26.** The efficiency for gas flow rates up to 12,500 scf/D is very close to that for water. A worse scenario could probably be imposed by assuming an adiabatic compression for the gas rather than the isothermal, as done here.

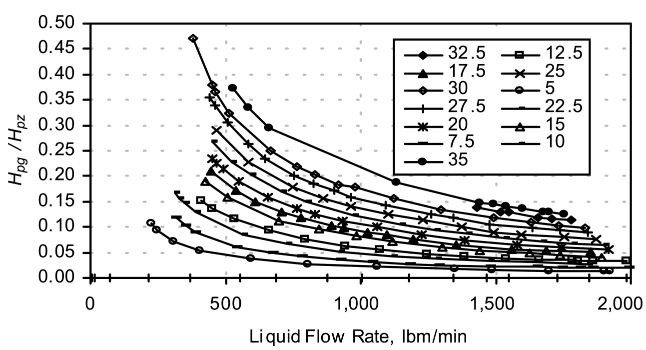

Fig. 22—Gas-to-liquid hydraulic horsepower ratio for Stage 3.

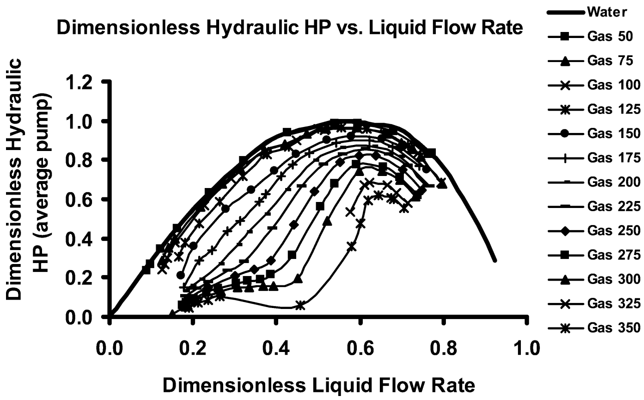

Fig. 23—Average hydraulic horsepower for the pump (isothermal gas compression).

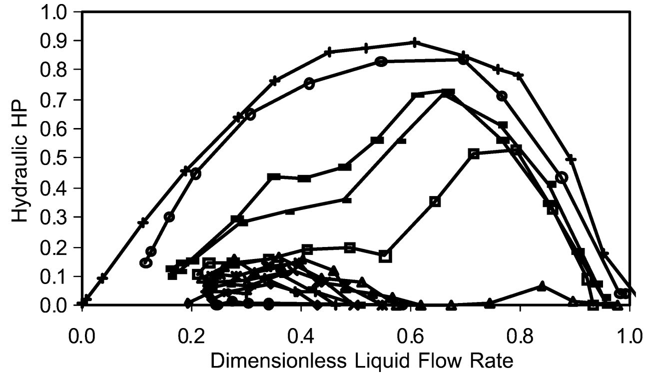

Fig. 24—Total hydraulic horsepower for Stage 1 at different gas flow rates.

The best-efficiency point of the pump moves to the right as gas flow rate increases, exactly as the surging maximum does. The two areas mentioned previously between the surging and gas-lock conditions are clearly defined for gas flow rates of greater than 17.5 Mscf/D. The brake-horsepower measurement for each stage is a challenge, but efficiency could be an interesting correlation parameter, if possible.

Further investigation is also required to establish whether the gas behaves isothermally, adiabatically, or maybe polytropically.

Conclusions

1. The petroleum industry lacks a general model to predict ESP performance under two-phase flow conditions.
2. Published gas-degradation and surging-prediction correlations are pump-specific because they are based on an average performance for a certain number of stages.
3. Single- and two-phase performance data were obtained for 22-stage mixed-flow-type pump stages at an intake pressure of 100 psig.
4. Average single- and two-phase performance data were obtained for the 22-stage, mixed-flow-type pump at a 100-psig intake pressure.
5. The average behavior of the pump is significantly different from that observed for each stage.
6. Further investigation is required regarding the behavior of the first stage before coming to any conclusions about it.
7. As the gas flow rate increases, the surging condition moves progressively from upstream to downstream stages.
8. The gas-to-liquid horsepower-compression ratio was as much as 0.45 (assuming an isothermal gas compression).
9. The average best-efficiency point of the liquid flow rate increases as the gas flow rate increases.
10. A second slope-change region in the pressure flow-rate curve was observed for low liquid flow rates.
11. The pressure increment and total hydraulic horsepower behavior is different for each stage.
12. Current knowledge is not sufficient to develop a general and accurate model for predicting head degradation, gas lock, and surging conditions.

Recommendations

1. The reasons for the observed pressure drop between pump suction and the first stage intake must be investigated.
2. Moving the sensor installed at the pump intake closer to the first stage or installing an additional sensor at that location is recommended. This way, intake losses can be measured for two-phase flow conditions with acceptable accuracy.
3. It is recommended that experiments continue for pump-intake pressures greater and less than 100 psig to investigate the effect of this parameter on ESP stage performance.
4. Explore the possibility of measuring the brake horsepower for each stage.
5. Use only new stages in future experiments to avoid additional uncertainties.
6. Reduce the pressure drop downstream of the pump, allowing a wider range of test conditions.

Nomenclature

a = correlation parameter from Romero[6]
$a_{1,2}$ = correlation parameters from Turpin[2]
B_{HP} = brake horsepower, hp
e = exponential function, $f(x)=e^x$
R_F = free-gas/liquid ratio, dimensionless
g = gravitational constant, 32.17 ft/sec^2
H = head, ft
k = ratio of specific heats (1.4 for air as an ideal gas)
$K, E1, E2, E3$ = constants developed by regression analysis,[8] dimensionless
$\dot{m}$ = mass flow rate, lbm/min

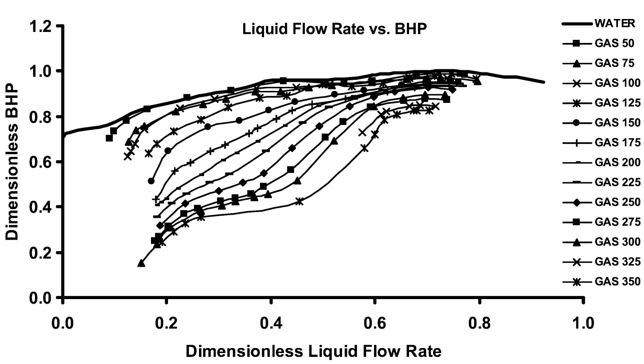

Fig. 25—Average brake horsepower for the pump.

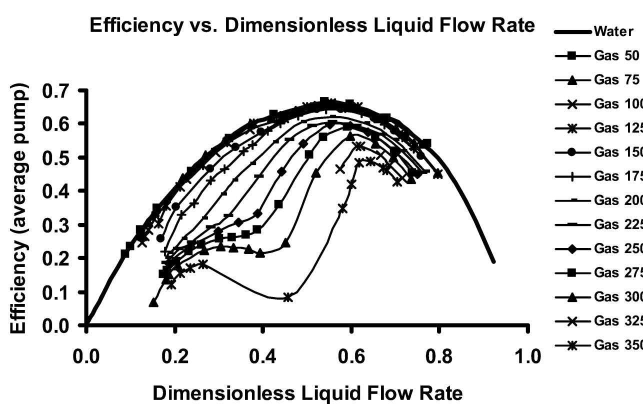

Fig. 26—Average efficiency for the pump (isothermal gas compression).

M = air molecular weight, 28.97 lbm/lb-mol
n = number of stages, dimensionless
p = pressure, psia
q = volumetric flow rate, B/D
Q = correlation parameter, B/D
R = ideal gas constant, 10.7316 psi-ft^3/(lb-mol °R)
T = temperature, °R
α = slip gas void fraction, dimensionless
γ_g = specific gravity, dimensionless
Γ = shaft torque, lbf-in.
Δp = pressure difference, psi
ε = efficiency, %
λ = non-slip gas void fraction (free gas fraction), dimensionless
ρ = density, lbm/ft^3
ϕ = correlation parameter from Turpin[2]
ω = angular speed, rpm

Subscripts

1 = initial condition
2 = final condition
d = dimensionless
$d$lim = dimensionless limit
$d$max = dimensionless maximum
g = gas
i = pump intake
l = liquid
m = mixture
SP = single phase
TP = two-phase
w = water

Superscripts

a = correlation parameter from Turpin[2]
adb = adiabatic thermodynamic process
discharge = pump discharge conditions
intake = pump intake conditions
isoth = isothermal thermodynamic process
k = adiabatic exponent for gas, dimensionless
max = maximum
SC = standard conditions (14.7 psia, 60°F)

Acknowledgments

The authors thank PDV-Intevep, Tulsa Artificial Lift Projects (TUALP) and its member companies—AGIP, Pemex, BP plc, ONGC, INTEVEP, and Shell—for sponsoring this work. Special thanks to Centrilift for donating the submersible pump tested in this work. We are also grateful to our technicians and assistants for their help.

References

1. Lea, J.F. and Bearden, J.L: "Effect of Gaseous Fluids on Submersible Pump Performance," *JPT* (December 1982) 2922.
2. Turpin, J.L., Lea, J.F., and Bearden, J.L.: "Gas-Liquid Flow Through Centrifugal Pumps-Correlation of Data," paper presented at the 1986 3rd Intl. Pump Symposium, Texas A&M U., May.
3. Dunbar, C.E.: "Determination of Proper Type of Gas Separator," paper presented at the 1989 Microcomputer Applications in Artificial Lift Workshop sponsored by the SPE Los Angeles Basin Section, October.
4. Cirilo, R.: "Air-Water Flow Through Electric Submersible Pumps," MS thesis, U. of Tulsa, Tulsa (1998).
5. Pessoa, R. *et al.:* "Tapered Pump Experimental Tests With Light and Heavy Oil in PDV INTEVEP Field Laboratory," paper presented at the 1999 SPE ESP Workshop, 28–30 April.
6. Romero, M.: "An Evaluation of an Electric Submersible Pumping System for High GOR Wells," MS thesis, U. of Tulsa, Tulsa (1999).
7. Sachdeva, R.: "Two-Phase Flow Through Electric Submersible Pumps," MS thesis, U. of Tulsa, Tulsa (1988).
8. Sachdeva, R., Doty, D.R., and Schmidt, Z.: "Performance of Axial Electric Submersible Pumps in Gassy Well," paper SPE 24328 presented at the 1992 SPE Rocky Mountain Regional Meeting, Casper, Wyoming, 18–21 May.
9. Furuya, O.: "An Analytical Model for Prediction of Two-Phase (Non-Condensable) Flow Pump Performance," *J. of Fluids Engineering* (1985) **107**.
10. Murakami, M. and Minemura, K.: "Effects of Number of Blades," second report, *Bull. of JSME* (1974) **17,** No. 112, 1286.
11. Wilson, B.L.: "ESP Gas Separator's Effect on Run Life," paper SPE 28526 presented at the 1994 SPE Annual Technical Conference and Exhibition, New Orleans, 25–28 September.
12. Zakem, S.: "Determination of Gas Accumulation and Two-Phase Slip Velocity in a Rotating Impeller," paper presented at the 1981 ASME Cavitation Forum.
13. *RP 11S2, Recommended Practice for Electric Submersible Pump Testing,* second edition, API, Washington, D.C. (1997).

SI Metric Conversion Factors

°API	141.5/(131.5+°API)		= g/cm^3
bbl ×	1.589 873	E–01	= m^3
ft ×	3.048*	E–01	= m
ft^3 ×	2.831 685	E–02	= m^3
°F	(°F–32)/1.8		= °C
hp ×	7.460 43	E–01	= kW
in. ×	2.54*	E+00	= cm
lbm ×	4.535 924	E–01	= kg
°R	(°R × 5/9)		= °K

*Conversion factor is exact.

Rui Pessoa is currently a research engineer in the Integrated Production Dept. at the Petróleos de Venezuela's (PDVSA) Research and Development Center (INTEVEP). He has been involved in many projects related with ESPs including research, installation, optimization, and diagnosis. His activities have focused on pump performance with viscosity and two-phase (gas-liquid) mixtures, rotary gas separator efficiency, and gas handling capabilities of ESPs. Pessoa holds BS and MS degrees in petroleum engineering from the U. Central de Venezuela and the U. of Tulsa, respectively. **Mauricio G. Prado** is assistant professor of the Petroleum Engineering Dept. of the U. of Tulsa and Director of TUALP—Tulsa U. Artificial Lift Project, an industrial academic cooperative research consortium formed in 1983 to conduct research on artificial lift. Prado holds a BS degree in metallurgical engineering from Inst. Militar de Engenharia, a MS degree in petroleum engineering from the U. Estadual de Campinas, and a PhD degree from the U. of Tulsa.